



NOVA

University of Newcastle Research Online

nova.newcastle.edu.au

Tran, Quang Anh; Stanger, Rohan; Xie, Wei Xie; Smith, Nathan; Lucas, John; Wall, Terry. "Linking thermoplastic development and swelling with molecular weight changes of a coking coal and its pyrolysis products". Published in Energy and Fuels Vol. 30, Issue 5, p. 3906-3916 (2016)

Available from: <http://dx.doi.org/10.1021/acs.energyfuels.6b00324>

This document is the Accepted Manuscript version of a Published Work that appeared in final form in Energy and Fuels, copyright © American Chemical Society after peer review and technical editing by the publisher. To access the final edited and published work see <http://dx.doi.org/10.1021/acs.energyfuels.6b00324>

Accessed from: <http://hdl.handle.net/1959.13/1348988>

1 Linking thermoplastic development and swelling
2 with molecular weight changes of a coking coal and
3 its pyrolysis products

4 *Quang Anh Tran*^{*a}, *Rohan Stanger*^a, *Wei Xie*^a, *Nathan Smith*^b, *John Lucas*^a, *Terry Wall*^a

5 ^aChemical Engineering, the University of Newcastle, Callaghan, NSW 2308, Australia

6 ^bAnalytical & Biomolecular Research Facility, the University of Newcastle, Callaghan, NSW 2308,
7 Australia

8 * Corresponding author. Email: quanganh.tran@uon.edu.au

9 **Abstract**

10 The thermoplastic development of an Australian coking coal was investigated by linking thermal swelling
11 with changes in molecular weight of its pyrolysis products. Coal thermal swelling was investigated
12 together with volatiles evolution and characterisation of generated volatiles (including volatile tar and
13 light gases). The molecular weight distributions of coal and its solvent extracts were measured by using
14 Laser Desorption/Ionization Time of Flight Mass Spectroscopy (LDI-TOF-MS). Solvent extraction (by
15 acetone and tetrahydrofuran (THF)) was initially used on the raw coal to aid interpretation of thermo-
16 swelling by volumetric expansion measurements. The removal of ~2% solvent soluble matter from the
17 raw coal (the mobile phase) reduced its swelling extent during heating by up to 22% (from 86% down to
18 68% and 64% for acetone- and THF- residues, respectively). Volatile release after solvent treatment
19 remained unaffected. This suggested that the majority of the coal's swelling behaviour could be attributed
20 to the formation of heat-generated liquid matter (the metaplast) during pyrolysis.

21 Broad molecular weight changes were found in the solvent extractable component (metaplastic material
22 extracted by acetone and THF) of the semi-coke. Prior to softening (350°C), the extractable components
23 were composed of molecules mainly <500 Da. The upper limit in molecular weight distribution of solvent
24 extracts increased significantly to 1800 Da at the onset of swelling (400-450°C) and decreased back to
25 ~500 Da at the end of swelling (500°C). The spectra showed that the volatile tar and acetone extract (the
26 light solvent extract) consisted of similar repeating structures separated 12-14 Da apart. As the treatment
27 temperature increased, the molecular weight distribution of volatile tar increased in molecular mass
28 approaching that of the acetone extract distribution (~600 Da). THF extract molecular weight distribution
29 was a mixture of 12-14 Da and 24 Da repeating units which only became apparent at molecular weight
30 above 600 Da.

31 The LDI-TOF-MS analysis of the solid coal showed that it contained a distribution of molecular
32 structures centred at 2000 Da and spanning between 500 and 7000 Da. This raw coal spectrum also
33 contained multiple repeating mass lines every 24 Da apart. Overall, these results suggested that the coal
34 consisted of complicated structures which subsequently degraded into smaller fragments capable of
35 forming a complex intermediate liquid phase and a distribution of lighter volatile tar species.

36

37 **Keywords:** Coal thermoplasticity; Solvent extraction; Metaplast

38

39 **1 Introduction**

40 *1.1 Coal thermoplasticity*

41 The transformation of coal to coke during coking is governed by the coal's thermoplastic behaviour.

42 During heating, the thermoplastic process includes softening, bubble formation, swelling, and eventually

43 resolidification at higher temperatures.¹ The result of this process is that discrete coal particles are
44 transformed into coke, a solid porous carbon residue that can act as a fuel, a chemical reducing agent, and
45 a high-strength permeable support during blast furnace operation.^{2, 3} The most common tests that can be
46 used to determine coal plastic properties include Gieseler plastometer and Arnu dilatometer.¹ Although
47 these two tests can be used to provide standardised information for empirical coal plasticity evaluation,
48 they do not provide an understanding of the underlying chemical changes that lead to bulk physical
49 transformation, nor do they adequately describe the actual thermoplastic behaviour in a coke oven.

50 *1.2 Coal chemical structure and its devolatilisation models*

51 In general, coal is envisaged to have a macromolecular network structure which consists of chains of
52 aromatic and hydro-aromatic structures cross-linked with aliphatic and ether bridges.⁴⁻¹⁰ The coal network
53 is highly porous and contains low molecular weight organic molecules known as the mobile phase¹¹ that
54 can be extracted by organic solvents.^{12, 13} To explain and predict product compositions generated during
55 pyrolysis, different coal network models have been developed. These network models include the
56 FLASHCHAIN model;¹⁴ the functional group – depolymerisation, vaporization and cross-linking (FG –
57 DVC) model;¹⁵ the chemical percolation devolatilisation (CPD) model.¹⁶ All three models include
58 network modelling, coal structure characterisation, depolymerisation reactions, cross-linking reactions,
59 and non-condensable gas, tar, and char formation. The differences among these models lie in their
60 chemical assumptions for devolatilisation mechanisms and mathematical approaches.¹⁷ These network
61 models have been developed with the intention of supporting coal behaviour prediction during
62 combustion processes which involves rapid devolatilisation of coal particles. However, coking coal
63 pyrolysis occurs at a slow and uniform heating rate, approximately 3-5°C/min in a coke oven.¹⁸
64 Therefore, modifications are needed for the prediction of coking coal behaviour and coke strength
65 development. A more fundamental understanding of thermoplasticity phenomena, including both
66 chemical and physical changes, is needed to optimise these coking coals for commercial utilisation,¹⁹ in
67 particular blend design in coke ovens which is currently still empirically based.

68 1.3 Coal metaplast

69 There are a number of hypotheses and theories that have been proposed to chemically explain coal
70 thermoplasticity.²⁰ Among them, the most noticeable theories are: the γ -fraction theory²¹ and the
71 metaplast theory^{6, 22, 23}. The difference between the two theories is that the former assumes softening
72 material is present in the raw coal, while the latter assumes that it is thermally generated. Based on the
73 metaplast theory, the metaplast refers to the fraction that does not immediately evaporate either to the
74 particle surface or into bubbles dispersed throughout the molten coal during pyrolysis.^{23, 24} The extent of
75 metaplast formation is determined by competition between volatilisation of the lighter material,
76 thermolysis rates of the coal macromolecular structure, and retrogressive rates that lead to solid
77 formation.²⁵ The metaplast is thought to be thermally unstable and it can decompose to form volatiles
78 and/or be transformed into coke.²² During coking coal pyrolysis, the amount of metaplast increases at first
79 and subsequently decreases. The metaplast can be isolated by rapidly cooling the coal after heating and
80 treating it with a solvent.¹ In practice, the choice of solvent will determine the largest structures removed
81 during this extraction process. Molecular weights up to 1,000,000 Da have been observed in solvent
82 extracts from semi-cokes using CS₂/NMP.²⁶ However, by using tetralin (a well-known hydrogen donor) in
83 a high-temperature solvent extraction (350°C), the metaplast was judged to correspond to the compounds
84 of <800 Da in molecular weight.²⁷

85 The amount of solvent-soluble constituents increased greatly at the fluidity stage and then decreased
86 towards resolidification stage, which suggested that solvent-soluble constituents were related to fluidity
87 behaviour.²⁸ Recently, Takanohashi et al.²⁶ stated that the fluidity of coking coal was determined by both
88 the components that present in raw coal (γ -fraction) and the components that were generated during
89 heating (metaplast). Based on this study on solvent extraction of heat-treated coals, they proposed a
90 “continuous self-dissolution model” in which the lighter molecular weight components (such as γ -
91 component, chloroform-soluble) should act as a solvent that can dissolve heavier molecular weight
92 components during heating. Such continuous dissolution is needed for coal softening and fluidity during

93 carbonisation.²⁸ Both physical and chemical changes during coal pyrolysis contributed to its fluidity
94 property, however, the nature of these changes and their effect on fluidity are not well understood.²⁸
95 This present work focuses on linking thermal swelling extent and volatiles evolution with changes in
96 molecular weight distribution of coal and its solvent extracts at different points during pyrolysis. The
97 swelling extent was analysed by Computer Aided Thermal Analysis (CATA), a novel technique that can
98 measure coal thermal and swelling behaviour simultaneously. In addition to total volatiles evolution
99 recorded by Thermogravimetric Analysis (TGA), Dynamic Elemental Thermal Analysis (DETA) was
100 utilised to quantify volatile tar and light gases evolution based on elemental carbon content. Solvent
101 extraction was undertaken on the semi-cokes prepared at different final pyrolysis temperatures between
102 350 and 600°C. The molecular weight distribution of coal and the solvent extracts was obtained by using
103 Laser Desorption Ionization- Time of Flight- Mass Spectrometry (LDI-TOF-MS) technique.

104

105 **2 Experiments**

106 *2.1 Coal sample*

107 An Australian coking coal was wet-sieved to 100-210 µm prior to testing. Coal petrographic analysis on
108 the single coal size fraction was performed using standard ISO 7404/5.²⁹ Petrography results with
109 proximate and ultimate analyses are given in Table 1.

110

Table 1: Properties of the investigated coal

Analytical techniques	Components	Proportion (%)
Proximate analysis	Ash	9.8
(wt%, db)	Volatile matter	23.7

	Fixed Carbon	66.5
	C	89.13
Ultimate analysis	H	4.24
(wt%, daf)	N	1.95
	O+S	4.68
Petrographic analysis	R_{vMax}^*	1.32
(mmf)	Vitrinite	55.6
	Inertinite	44.4
	Telovitrinite	50.7
	Detrovitrinite	2.7
Maceral components	Semifusinite	40
(%)	Fusinite	1.3
	Inertodetrinite	1.3
	Mineral matter	4

* *Mean Maximum Reflectance*

111

112

113 2.2 *Thermogravimetric analysis*

114 Thermogravimetric analysis (TGA) was performed on the coking coal and its Soxhlet extraction residues
 115 using thermogravimetric analyser Q50 manufactured by TA instrument. To analyse sample mass loss
 116 during pyrolysis, about 10 mg sample was heated from room temperature to 100°C using 20°C/min
 117 heating rate and held at this temperature for 10 minutes to remove excess solvents and moisture. The
 118 sample was then heated to 1000°C with 5°C/min increment under nitrogen atmosphere (50 ml/min flow
 119 rate). When the sample temperature reached 1000°C, 50 ml/min air flow was supplied into the heating
 120 chamber to oxidise the remaining coke for 30 minutes. Ash yield collected at the end of TGA experiments
 121 were used for the calculation of extraction yield via ash tracer method.³⁰

$$W = \frac{10^4(A_1 - A_0)}{A_1(100 - A_0)} \quad (1)$$

122 where W is the extraction yield (% , dry basis), A₀ is the ash content of the raw coal (% , dry basis), and A₁
123 is the ash content of the solvent residue (% , dry basis).

124

125 2.3 Computer Aided Thermal Analysis

126 Computer Aided Thermal Analysis (CATA) was employed to examine coal swelling behaviour during
127 pyrolysis. Approximately 2 g of coal was packed into 11.07 mm ID quartz tube at a density of ~950
128 kg/m³. The *swelling ratio* was determined by transient change in the length of the coal pellet which was
129 measured by a linear variable differential transformer (LVDT) during pyrolysis:

$$\text{Swelling ratio} = \frac{\Delta L}{L_0} \times 100\% \quad (2)$$

130 Where ΔL is the transient change measured by the LVDT, L₀ is the length of the packed coal pellet (~20
131 mm). In CATA experiments, duplicate runs were conducted with the weight variation was controlled to
132 be <0.1 g and acceptable deviation in maximum swelling extent was <3%. For swelling comparison
133 between raw coal and its solvent residues in this work, the difference in utilised weight was recorded at
134 ~0.05 g while ~0.02 g was the weight difference recorded between two residues. In addition to thermal
135 swelling, thermal *swelling rate* was also calculated to gain insight into phenomenon occurred during
136 plastic range. To achieve this goal, the swelling rate was obtained as the first derivative of thermal
137 swelling profile.

138 During CATA experiments, 30 ml/min argon flow was supplied into the heating chamber to carry
139 generated volatiles out of the coal pellet. As coal was heated at 5°C/min rate, the upstream inlet gas
140 pressure was also measured. The inlet gas pressure has been shown previously to correspond with
141 changes in bed permeability during coal softening. The difference in pressure between the front-end and

142 back-end of the coal pellet was assigned as the pressure drop (ΔP). The significant increase in pressure
143 drop value ($\Delta P > 2$ kPa) was taken as the swelling onset point. Details of the CATA technique can be
144 found elsewhere.³¹⁻³³

145 **2.4 Dynamic Elemental Thermal Analysis**

146 Dynamic Elemental Thermal Analysis (DETA) was utilised to investigate the evolution of total volatiles,
147 dynamic tar, and light gases during coal pyrolysis. Samples were heated from room temperature to 800°C
148 using 5°C/min heating rate under inert atmosphere generated by argon flow. The volatiles were
149 combusted using a custom heated O₂ lance downstream of the coal sample with combustion products
150 (CO₂/CO, H₂O, H₂, NO_x, SO_x, and O₂) measured at the furnace exit after cooling. These measurements
151 enable the calculation of elemental composition of the volatiles during pyrolysis and are referred to as
152 Total-Volatiles mode. Light-Gases operation mode operated with the O₂ lance placed in a second
153 chamber. An iced tar condenser was placed between the heating furnace and the second combustion
154 chamber. The “tar by difference” was calculated by subtracting light gases from total volatiles
155 measurement. Solid residue (coke) was combusted after pyrolysis by supplying an additional flow of
156 oxygen into the system when the sample temperature reached 800°C. The working principal of this
157 technique is outline elsewhere.³⁴⁻³⁶

158 **2.5 Solvent extraction**

159 Acetone and tetrahydrofuran (THF) were used for solvent extraction studies. Between these two solvents,
160 acetone was considered to be weaker than THF since the difference between acetone electron donor
161 number (DN=17) and its electron acceptor number (AN=12.5) was +4.5, lower than that in THF which
162 was reported to be +12 (DN=20, AN=8).³⁷ The choice of THF as the “heavier” solvent to study metaplast
163 is derived from previous researchers’ opinions on the formation of “colloidal dispersions” which could
164 bias the molecular weight measurements.³⁸ This phenomenon has been observed in asphaltenes.³⁹ Two
165 types of solvent extraction were used in this study: conventional Soxhlet extraction and multi-stage
166 solvent extraction.

167 Soxhlet extraction was conducted on raw coal to inspect the change in coal swelling behaviour after it had
168 been exhaustively extracted by organic solvents. The second type of extraction was multi-stage solvent
169 extraction performed under room temperature to investigate the variation in molecular weight distribution
170 (MWD) of solvent extracts obtained from raw coal and preheated semi-coke samples.

171 *Soxhlet extraction*

172 About 5g coal was put in a quartz thimble which was then inserted in the Soxhlet extraction apparatus.
173 Heating power was adjusted so that a 20 min/cycle reflux was applied to both acetone- and THF-
174 extraction in 24 h. In both cases, the refluxed solvent became colourless before this 24-hour mark was
175 achieved. Solvent extraction residues were removed from the quartz thimble, dried under vacuum for 24
176 h, before being subjected to swelling behaviour (CATA) and volatiles release (TGA) investigation.

177 *Multi-stage solvent extraction*

178 Multi-stage batch extraction was conducted in the first stage by extracting coal and semi-coke (heated
179 coal sample) with ~200 mL acetone. After 72 h with regular stirring, the solid residue was removed and
180 added ~200 mL distilled THF for second stage extraction. This process was performed sequentially at
181 room temperature rather than using Soxhlet extraction technique to avoid any possible impacts of boiling
182 solvent on the thermally unstable extracts (the metaplast). Acetone-soluble fraction (Acetone extract) and
183 THF-soluble fraction (THF extract) were products of this approach and were used to obtain information
184 on the changes of their molecular weight distributions (MWD) at different pyrolysis temperatures. Since
185 the aim of this work was to observe changes in MWD of pyrolysis products, solvent extraction yield was
186 not acquired.⁴⁰

187

188 **2.5.1 Preparation of heat treated semi-cokes prior to solvent extraction**

189 About 500 mg coal was heated in a Sinku Riko infrared gold image furnace to temperatures between
190 350°C and 600°C using 5°C/min heating rate. Products of the heat-treatment process were divided into
191 two components: semi-coke, the remained solid component; and volatiles, the gaseous component
192 vaporised during pyrolysis.

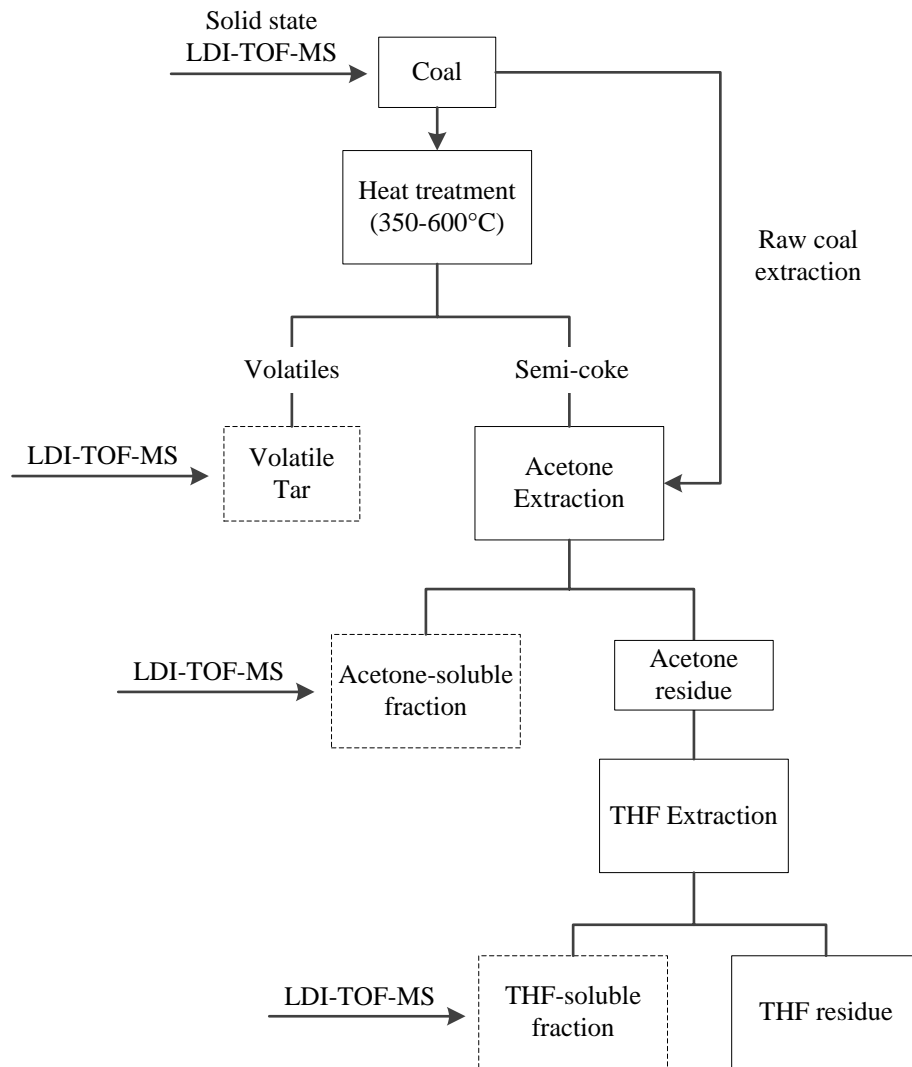
193 Generated volatiles were driven towards a downstream tar condenser by supplying 30 ml/min argon flow
194 into the heating chamber. The tar condenser was surrounded by ice in an insulation bucket. By doing so,
195 volatiles were further divided into volatile tar (condensable fraction); and light gases (non-condensable
196 fraction). Volatile tar was collected for further investigations by washing the condensable fraction with
197 acetone. Semi-cokes obtained from different pyrolysis temperatures were subjected to a multi-stage
198 solvent extraction process to generate solvent extracts which were then analysed by mass spectrometry.

199

200 **2.5.2 Laser Desorption Ionization- Time of Flight- Mass Spectrometry**

201 The extractable material (from raw coal and heat-treated samples) and the collected tar were analysed
202 using Laser Desorption Ionization- Time of Flight- Mass Spectrometry technique (LDI-TOF-MS). In
203 addition to solvent-soluble components, LDI-TOF-MS was also utilised to characterise MWD of solid
204 coal (solid state LDI-TOF-MS). The experimental scheme showing the derivation of generated LDI-TOF-
205 MS samples is outlined in Figure 1.

206



207

208

Figure 1: LDI-TOF-MS analysis scheme

209

210 The LDI-TOF-MS experiments were conducted on Bruker Daltonics UltrafleXtreme MALDI TOF/TOF
 211 Mass Spectrometer for both dissolved liquid extracts and solid samples. For liquid extract samples, a
 212 volume of 0.8 μL was deposited, matrix-free, onto a Ground Steel target plate and the solvent (acetone or
 213 THF) was allowed to evaporate at ambient temperature. For solid coal analysis, coal was ground for
 214 approximately 2 minutes prior to embedding the sample on the target plate. The solid coal sample was

215 deposited on 3M™ double sided electrical tape. Excess particles were removed from the targeting plate
216 by nitrogen flow and only particles held by the tape were subjected to solid LDI-TOF-MS analysis.

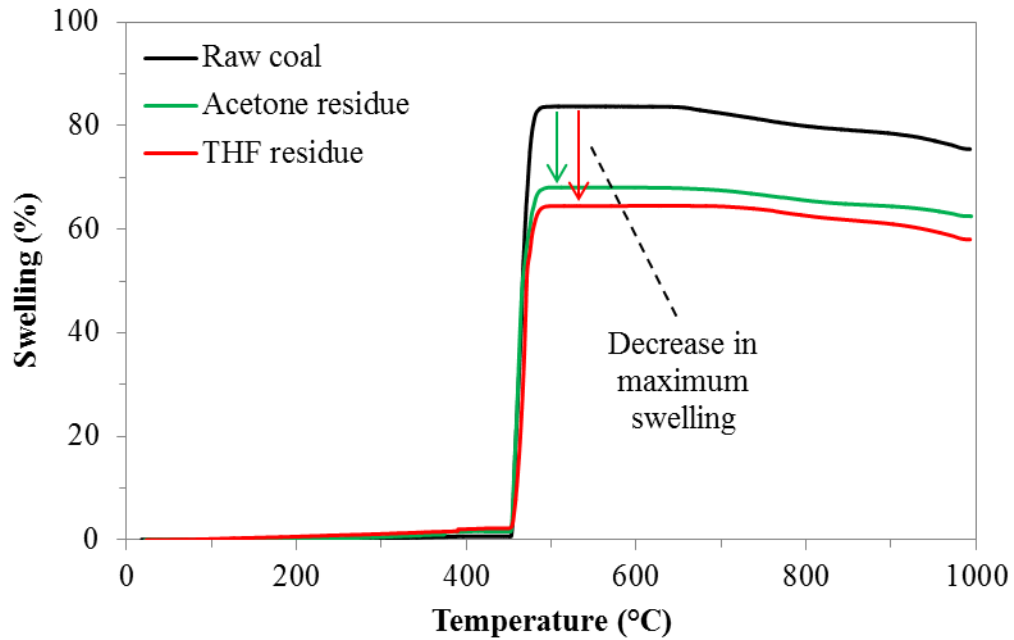
217 Samples were analysed using a smartbeam II laser (Nd:YAG, 335 nm) in positive, reflectron mode. A
218 total of 2000 laser shots were accumulated for each sample at 500 shot intervals from random positions in
219 the sample slot. Laser power was kept at 60% energy level for liquid sample and at 80% energy level for
220 solid coal sample. The detected mass was set from 20 to 7980 Da, the limitation of detector in reflectron
221 mode. The obtained spectra were presented for ions with molecular weight higher than 200 Da since
222 lower molecular weight compounds were generally considered as fragmentation of larger molecules
223 during ionisation. As a result, no further investigations were conducted on these lower molecular weight
224 materials. This LDI-TOF-MS operational mode and sampling scheme (except solid state analysis) have
225 been used to observe changes in solvent extracted material from heated coal in our previous work.⁴⁰

226 **3 Results**

227 *3.1 Thermal swelling behaviour*

228 The influence of solvent extraction prior to heating on coal thermoplasticity was evaluated for both
229 acetone and THF. Thermal swelling behaviour of raw coal and Soxhlet solid extraction residues was
230 obtained by CATA technique and is illustrated in Figure 2. Calculated coal swelling rate and pressure
231 drop profile of gas passing through raw coal on heating within the plastic range (400-600°C) are given in
232 Figure 3. Table 2 presents selective data obtained from CATA experiment on raw coal.

233

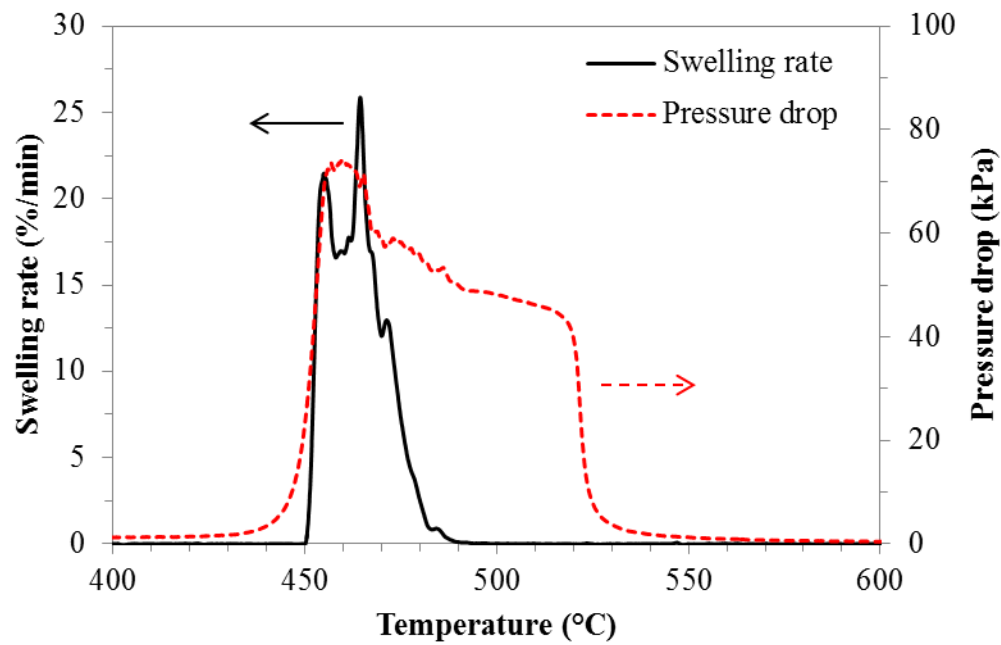


234

235

Figure 2: Thermal swelling behaviour of raw coal and Soxhlet solid extraction residues.

236



237

238

Figure 3: Thermal swelling rate and pressure drop of raw coal within the plastic range (400-600°C)

239

240

Table 2: Summary data from CATA experiments on raw coal

Temperature (°C)	Swelling rate (%/min)	Pressure drop (ΔP , kPa)	Phenomena
433	-	>2	Swelling onset
450	>1	-	Swelling acceleration
457	-	74	Maximum in pressure drop
464	26	-	Maximum in swelling rate
482	<1	-	Swelling stopped Maximum swelling: 83%
538	-	<2	No resistance on carrier gas
675	-	-	Contraction started, swelling percentage dropped from 83% to 82%

241

242 *Raw coal thermal swelling behaviour*

243 As the coal sample was heated, the packed coal pellet underwent dramatic changes in length (and
244 therefore volume). Changes in length of the packed pellet were first observed at 450°C (defined by
245 swelling rate exceeding 1 %/min). The rate of swelling then increased significantly, reaching its first peak
246 of 21 %/min at 455°C which coincided with the significant rise in pressure drop profile. The second peak,
247 maximum thermal swelling rate (26 %/min), was detected at 464°C. After this temperature, the rate of
248 sample volumetric expansion decreased dramatically with a shoulder peak recorded at 472°C. At 482°C,
249 swelling stopped and thermal swelling extent at this point was 83% compared to its initial packing length

250 at room temperature. This swelling rate profile was coal-specific and was expected to be influenced by
251 sample particle size.

252 The increase in pressure drop ($\Delta P > 2$ kPa) across the packed pellet, indicating softening onset, started at
253 about 430°C and was earlier than the detectable change in volumetric measurement at 450°C. The
254 maximum in pressure drop was measured at 457°C, slightly lower than the temperature at maximum
255 swelling rate (464°C).

256 Changes in pressure drop through the coal pellet occurred over a wider temperature range compared to
257 swelling rate. Specifically, the temperature at which the pressure drop value reduced back to smaller than
258 2 kPa after swelling was 538°C, while swelling had already stopped at 482°C. It is unclear at this point
259 why pressure drop and the end of swelling do not coincide. However, the pressure drop measurement may
260 be more sensitive to the beginning of high temperature contraction.

261 *Impact of coal extractable removal on thermal swelling behaviour*

262 A decrease in maximum swelling was observed in both Soxhlet extraction residues as shown in Figure 2.
263 While raw coal possessed a maximum swelling of 83%, this value was only 68% and 64% for acetone
264 and THF-residue, respectively. The fall in maximum swelling demonstrated the impact of a solvent
265 treatment step on its residues. Acetone, the weaker solvent, reduced 15% of coal maximum swelling
266 while this decrease in maximum swelling was 19% when THF, the stronger solvent, was used. Thus,
267 removing the soluble portion of the initial mobile phase in this coal can reduce the subsequent thermo-
268 swelling by up to ~22%.

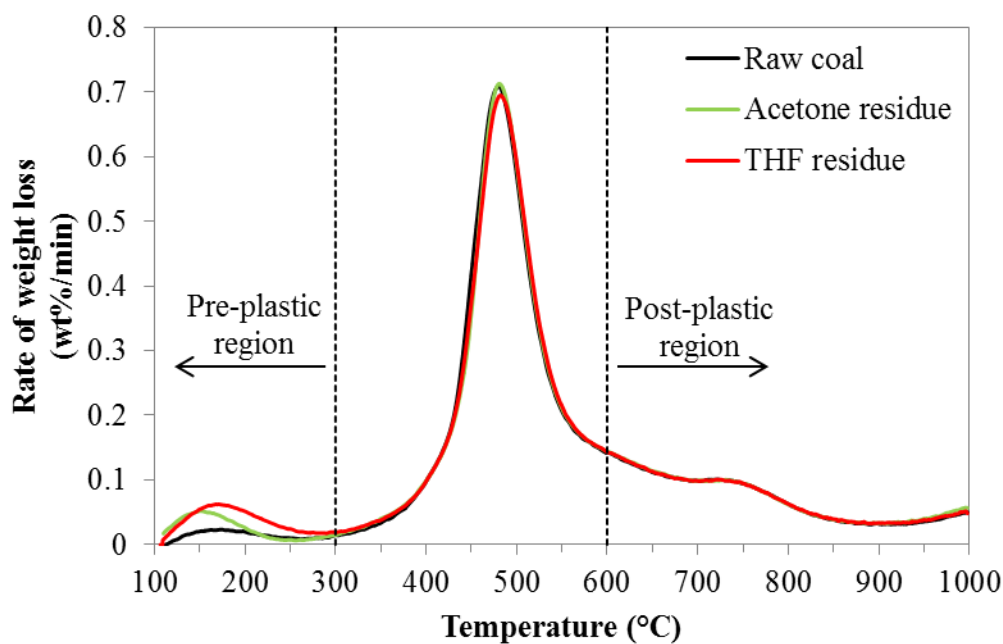
269 Although the coal had been exhaustively extracted by two different organic solvents, it is clear that the
270 removal of acetone- and THF-extracts from raw coal were not entirely responsible for the swelling
271 behaviour. This suggested that either the “mobile phase” was not entirely removed during solvent
272 extraction because it remained trapped in the coal network,^{41, 42} or that it is the heat-generated
273 components (the metaplast) that contributed the most towards coking coal swelling behaviour.

274

275 **3.2 Volatiles characterisation**

276 *Total volatiles evolution from coal and its solvent residues*

277 Raw coal and its Soxhlet extraction residues were analysed by TGA. Their devolatilisation profiles (DTG,
 278 Derivative Thermogravimetric Analysis) are shown in Figure 4 with summary data presented in Table 3.



279

280 **Figure 4: DTG profiles of raw coal and its Soxhlet extraction residues**

281

282 **Table 3: Summary data obtained from raw coal and Soxhlet extraction residues**

Sample	Volatile	Ash	Extraction	R_{Max}^b	T_{Max}^c	Weight loss
	matter	Coke				
	(wt%, dry)	(wt%, dry)	(wt%, db)	(wt%/min)	(°C)	(wt%, daf)

Raw coal	20.4	70.4	9.16	-	0.708	479	1.0
Acetone residue	21.9	68.7	9.34	2.09	0.713	481	1.8
THF residue	21.7	69.0	9.34	2.09	0.695	482	2.2

283 ^a *Calculated via as tracer method*

284 ^b *Maximum rate of weight loss*

285 ^c *Temperature at maximum rate of weight loss*

286 The DTG profile of raw coal shown in Figure 4 has been broadly divided into three different regions: pre-
 287 plastic region (<300°C), plastic region (300-600°C), and post plastic region (>600°C). Although the
 288 sample was held at 100°C for 10 minutes prior to being heated to 1000°C to remove excess solvents and
 289 moisture, it is clear that light compounds still vaporised in the pre-plastic region. These materials
 290 accounted for approx. 1% of weight loss during raw coal pyrolysis on dry-ash-free basis. Primary
 291 devolatilisation occurred in the plastic region with maximum rate of weight loss (R_{Max}) recorded at 479°C
 292 (T_{Max}). This temperature, interestingly, was close to the temperature at which coal swelling stopped
 293 (482°C, Table 2). In post-plastic region, coal continued to lose weight to the end of TGA experiment with
 294 a shoulder peak in DTG profile detected at around 750°C.

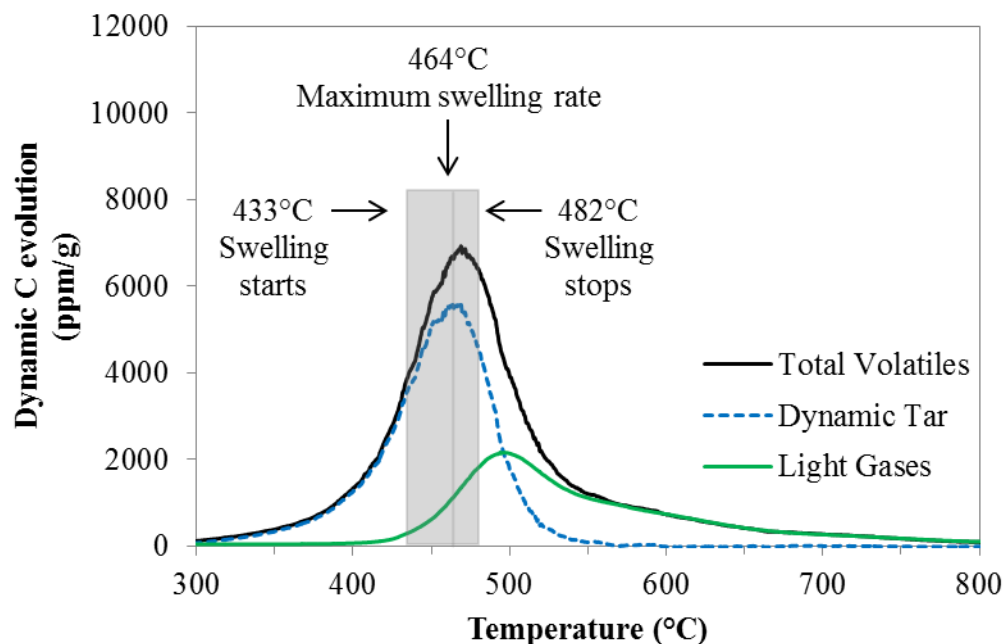
295 In the Soxhlet extraction residues, a similar decomposition trend was observed in both residues in all
 296 three regions. The decomposition of acetone residue ended at about 250°C, while THF residue continued
 297 to lose weight towards higher temperatures, leading to an overlap between its pre-plastic decomposition
 298 and primary devolatilisation in plastic region. For further investigation, weight loss up to 300°C of
 299 solvent residues was obtained. This comparison revealed that between 100 and 300°C, solvent residues
 300 decomposed more than raw coal. While raw coal lost only 1% weight loss in this region, this value in
 301 acetone- and THF-residues was 1.8 and 2.2%.

302 Extraction yield calculated by the ash tracer method (Eq. (1)) showed that both solvents only removed
303 about 2% of the initial mass on dry basis. Despite the the removal of only 2% of the coal mass through
304 solvent extraction, it is noted that this removal had a significantly higher impact on swelling. However,
305 the maximum swelling of residues was still considerable (68% and 64% for acetone- and THF-residues,
306 respectively), it is clear that the extractable components alone was not responsible for the bulk of thermal
307 swelling extent.

308 *Characterisation of volatiles evolved during raw coal pyrolysis*

309 Further characterisation of volatiles generated during raw coal pyrolysis was conducted by using
310 Dynamic Elemental Thermal Analysis (DETA), a novel technique that can differentiate dynamic tar and
311 light gases from total volatiles evolution. Dynamic changes are presented as the evolution of elemental
312 carbon and linked with key phenomena occurring in coal swelling profile as shown in Figure 5. Key
313 temperatures in DETA experiments are presented in Table 4. Results of DETA analysis in both total
314 volatiles and light gases mode are summarised in Table 5.

315



316

317

Figure 5: Dynamic carbon evolution during coal pyrolysis.

318

319

Table 4: Key temperatures in DETA analysis

	Carbon evolution start ^a (°C)	Carbon evolution peak (°C)	Carbon evolution completion ^b (°C)
Total volatiles	334	469	745
Dynamic Tar	330	463	536
Light gases	437	494	798

320

^a 1% of total carbon evolution between 300-800°C

321

^b 99% of total carbon evolution between 300-800°C

322

323

Table 5: Summary of coal DETA analysis

	C	H	N	S	O	Fractional split of volatiles released between 433-482°C (% volatile carbon)
	(%, daf)					
Total volatiles	12.84	4.09	0.27	0.00	-	-
Dynamic Tar ^a	7.39	2.71	0.23	0.00	-	83.5
Light gases	5.45	1.37	0.04	0.00	-	16.5
Coke	76.80	0.80	0.30	0.03	-	-
Total	89.64	4.89	0.57	0.03	4.87 ^a	-

324 ^a by difference

325

326 By integrating the volatile tar carbon evolution shown in Figure 5, it was found that the temperature
327 which corresponded to 1% of dynamic tar carbon evolution between 300-800°C was 330°C (Table 4).
328 This point was considered to be the start of tar evolution and was ~100°C earlier than the swelling onset
329 of coal pellet (433°C, Table 2). Tar evolution peaked at 463°C, just before the coal pellet reached its
330 maximum in swelling rate (at 464°C). The end point of tar evolution was found to be 536°C (Table 4) and
331 was just before to the point at which no resistance exerted on carrier gas as presented in Table 2.

332 The onset evolution of light gases began at 437°C and was close to swelling onset (Table 2). Light gases
333 evolution rate peaked at 494°C (Table 5). As a result, the maximum evolution of total volatiles at 469°C
334 could be mainly attributed to tar evolution. The evolution of tar completed at 536°C while light gases
335 continued to evolve out of the sample towards the end of DETA experiment. Combined with the pressure
336 drop profile in Figure 3, the sudden drop in ΔP between 520-530°C could be linked with the end of tar
337 evolution. In addition, as shown in Table 5, the amount of volatile tar evolved out of the coal was about
338 four times more than that of light gases within the swelling range (between 433 and 482°C). This

339 observation, once again, emphasised the important role of tar evolution and the build-up of its precursor
340 (the metaplast) on coal swelling behaviour.

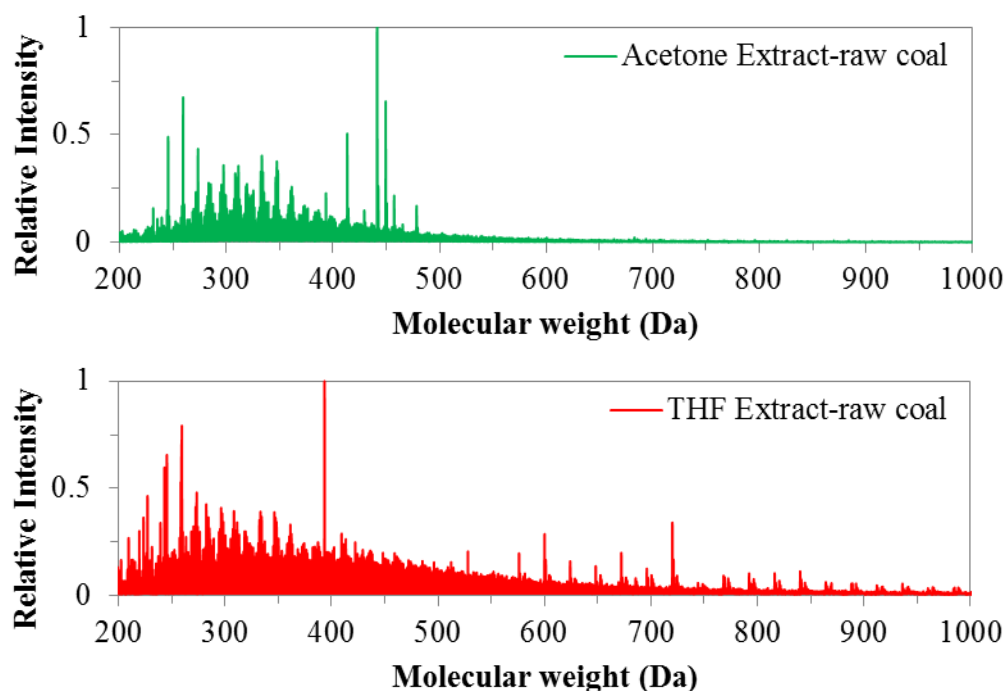
341

342 3.3 *Molecular weight distribution of coal and its pyrolysis products*

343 The LDI-TOF-MS technique was employed to analyse changes in molecular weight distribution (MWD)
344 of coal and its pyrolysis products. The pyrolysis products include vaporised component (volatile tar), and
345 extractable components (acetone- and THF-extract) from semi-coke.

346 3.3.1 **Raw coal extracts**

347 Multi-stage extraction was conducted on raw coal (no thermal treatment) to receive information on MWD
348 of coal extractable at room temperature (~20°C). Results are presented in relative intensity and shown in
349 Figure 6.



350

351 **Figure 6: Molecular weight distribution of coal solvent extracts at room temperature**

352

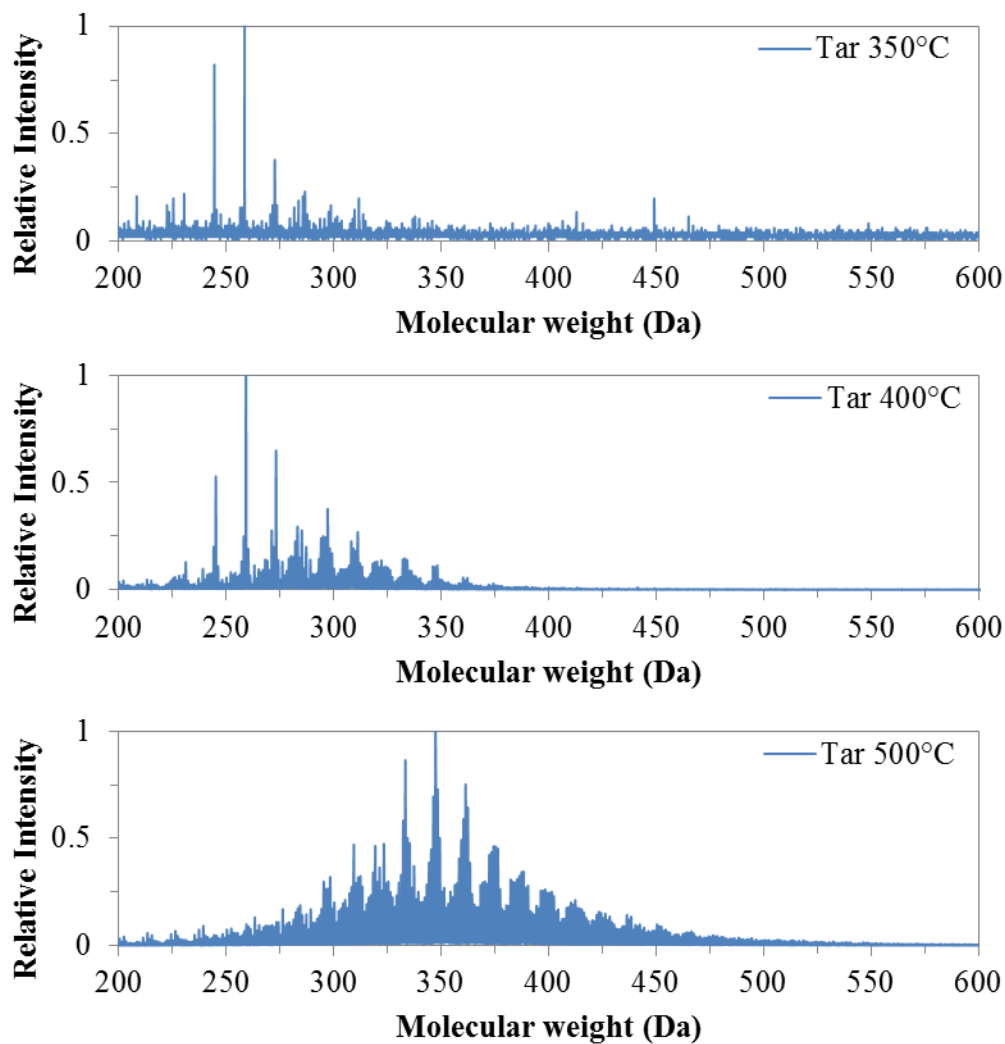
353 Acetone and THF-extract from coal both contained >200 Da materials. The upper limit in acetone extract
354 MWD was ~600 Da while this value in MWD of THF extract extended to ~1000 Da. The difference in
355 this upper limit is attributed to the difference in solvent strength. The 200-600 Da components were also
356 presented in THF extract after it had been previously extracted by acetone. This is likely due to the
357 limited solubilities of heavier compounds in acetone.

358 **3.3.2 Pyrolysis products**

359 *Volatile tar*

360 Volatile tars were collected during coal heat-treatment process. Their selected MWDs are illustrated in
361 Figure 7 at 350, 400, and 500°C. At 350°C, the volatile tar does not form any particular shape of
362 distribution and appears to contain a relatively small number of significant peaks. In addition, its low
363 intensity (maximum intensity: 95) coupled with the DETA results suggested that the amount of volatile
364 material formed at this temperature was low. As the pre-treatment temperature was increased from 350 to
365 500°C, there was a consistent increase in volatile tar molecular weight. At 400°C, the upper limit of
366 volatile tar MWD was about 400 Da. This value then increased up to about 600 Da as treatment
367 temperature reached 500°C.

368



369

370 **Figure 7: Changes in volatile tar molecular weight distribution as a function of treatment temperature**

371

372 *Semi-coke extracts*

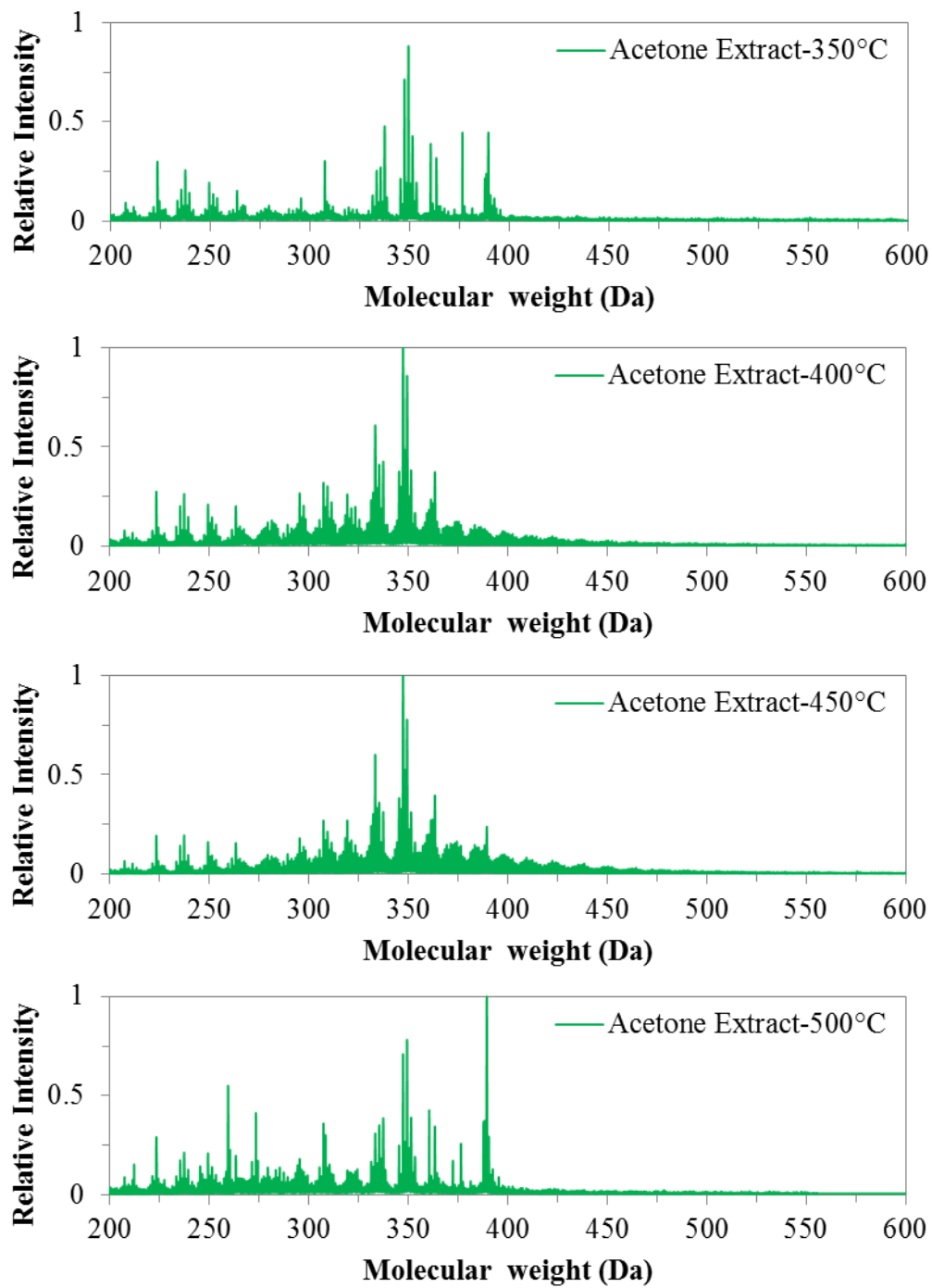
373 Selected spectra of acetone and THF extracts from pre-treated semi-cokes are presented in Figure 8 and

374 Figure 9, respectively. The acetone extracts showed relatively consistent molecular structures up to 500

375 Da were maintained in the coal during heating. These molecular structures are of similar range to the

376 volatile tar results and are consistent with previous work.⁴⁰

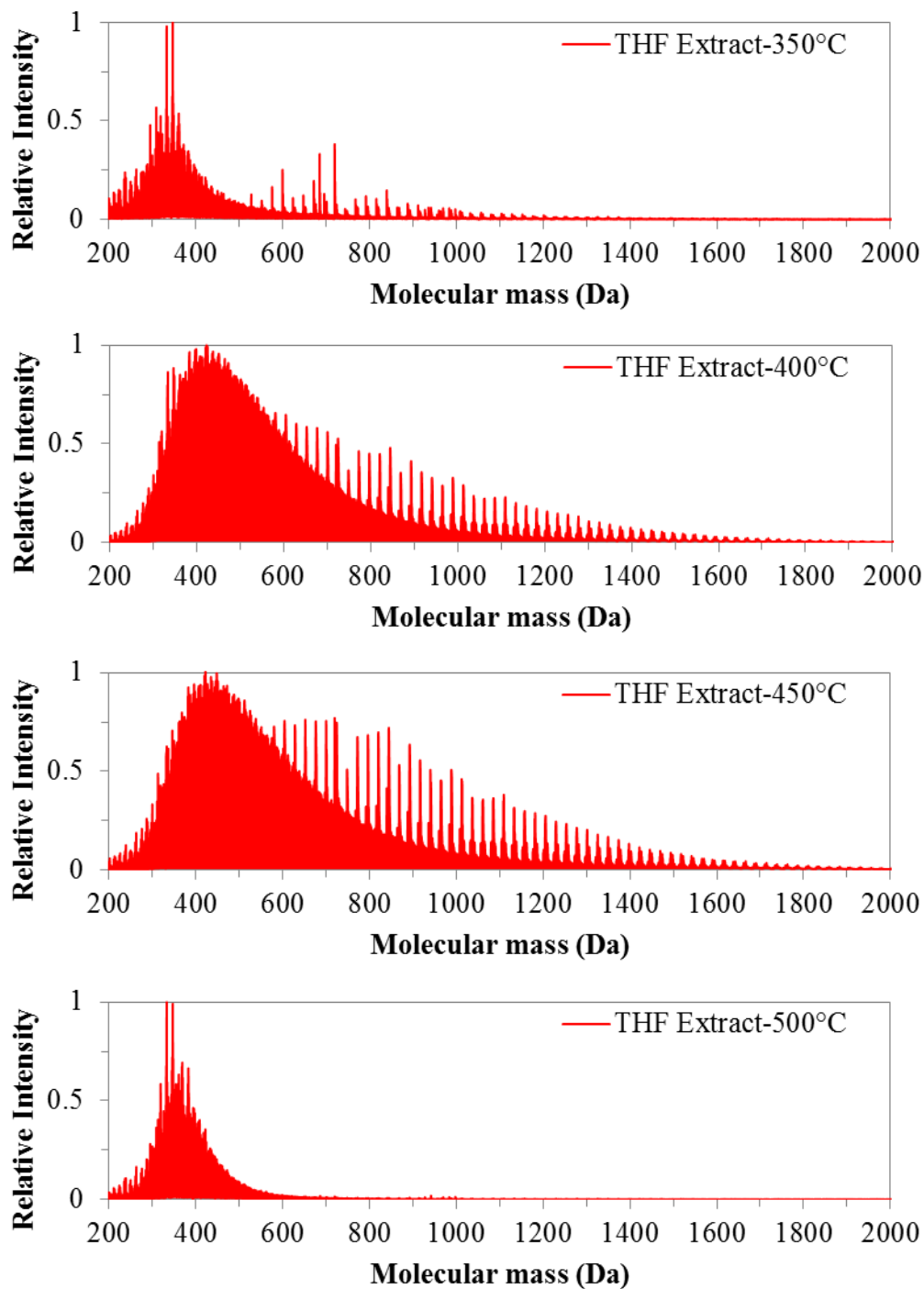
377 The THF extracts from the semi-coke displayed a significant sensitivity to temperature, changing from an
378 initial upper limit of 500 Da to up to 1800 Da and then back. The THF extract at 350°C (Figure 9)
379 possessed a MWD similar to THF extract from raw coal (Figure 6) with molecular class of compounds in
380 the range of 200-1000 Da. Such similarity did not exist between acetone extracts obtained at room
381 temperature and at 350°C. With increasing heat treatment temperature, there was an increase followed by
382 a subsequent decrease in MWD of acetone and THF extracts. Specifically, the upper limit in acetone
383 extracts at 400°C extended to about 500 Da. In comparison, THF extracts showed a significant expansion
384 in MWD at 400°C, and the inclusion of additional class of compounds that became apparent between 600
385 and 1800 Da with repeating peaks separated every 24 Da. The upper limit of these compounds decreased
386 from 1800 Da to about 600 Da at 500°C with the disappearance of the 600-1800 Da compounds.
387 Interestingly, THF extract MWD at 500°C was similar to spectrum of volatile tar collected also at this
388 temperature (spanning between 200 and 600 Da, Figure 7).



389

390

Figure 8: Changes in molecular weight distribution of acetone extracts from heated coal



391

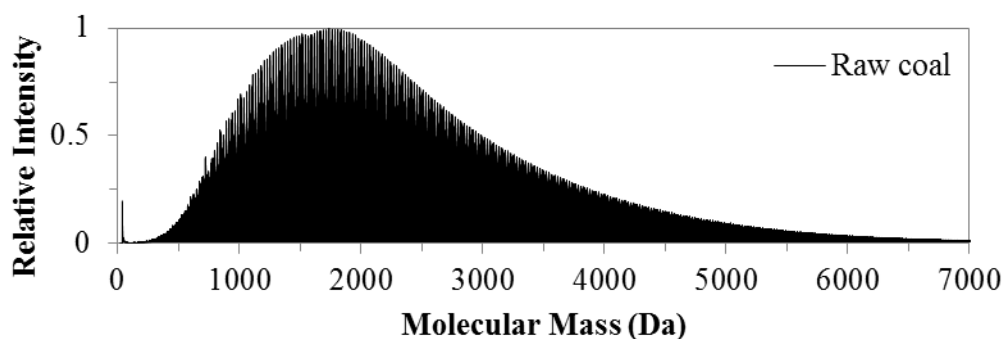
392

Figure 9: Changes in molecular weight distribution of THF extracts from heated coal

393

394 3.3.3 Solid state LDI-TOF-MS on coal

395 In addition to the investigation of pyrolysis products dissolved in organic solvents, LDI-TOF-MS was
396 also utilised to conduct studies on solid coal particles. The obtained spectrum from this solid state LDI-
397 TOF-MS experiment is presented in Figure 10.



398

399

Figure 10: Molecular weight distribution of raw coal

400 The solid coal spectrum displayed a right-skewed distribution with molecular weight spanning from 500
401 to beyond 7000 Da peaking between 1500 and 2000 Da. Because LDI-TOF-MS solid state analysis used
402 in this study was in Reflectron mode, it is clear that the obtained spectrum did not represent the entire coal
403 molecular structure, and that coal possessed a much more complex structure compared to its generated
404 pyrolysis products of which highest molecular weight only reached ~1800 Da. For further investigations,
405 bulk molecular weight distributions of coal and its pyrolysis products are viewed in detail in the next
406 section.

407

408 3.4 Interpretation of molecular weight spectra

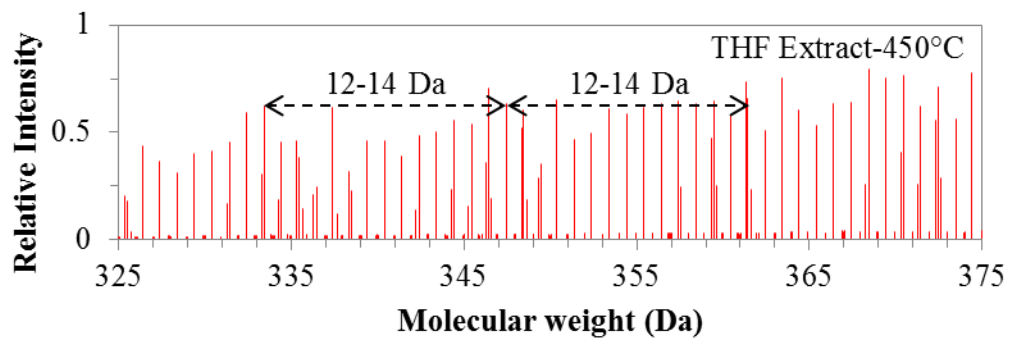
409 Previous sections provided an overview on solid coal particles and on changes in MWD of pyrolysis
410 products as a function of temperature. However, each obtained spectrum by itself contained information
411 that can only be analysed if the data is viewed at narrower MW scale. This incremental analysis was
412 conducted on both solid coal and its pyrolysis products and is presented in Figure 11 and Figure 12.

413 3.4.1 Pyrolysis products

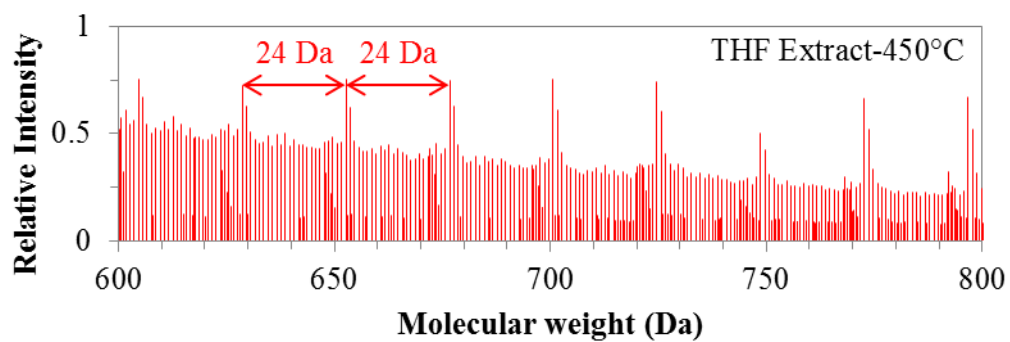
414 At narrower scales (e.g., between 325 and 375 Da), MWD of both volatile tar and acetone extract
415 contained repeating structures every 12-14 Da between peaks with each local peak group consisting of
416 satellite lines in a distribution on either side. Such behaviour was commonly observed by Herod et al.,⁴¹
417 Rodgers and Marshall,⁴² Nomura et al.,⁴³ and Stanger et al.,⁴⁰, and considered to be representative of
418 homologous series adding additional methyl groups (i.e., -CH₃) to a base aromatic unit. Figure 11 shows
419 an example for the THF extract prepared at 450°C.

420 The 12-14 Da repeating structure recorded in tar and acetone extract, though aligned to the same
421 molecular weight, was less pronounced in THF extract spectrum (Figure 11a) and could only be observed
422 in THF extract up to 600 Da. Individual peaks in volatile tar, acetone and THF extracts spectra at MW
423 <600 Da aligned to the same molecular weights, suggesting that the same chemical structures existed in
424 these pyrolytic products. Above 600 Da (Figure 11b), an additional group of peaks characterised by
425 repeating every 24 Da apart from each other emerged in THF spectrum.

426



(a) THF extract below 600 Da



(b) THF extract above 600 Da

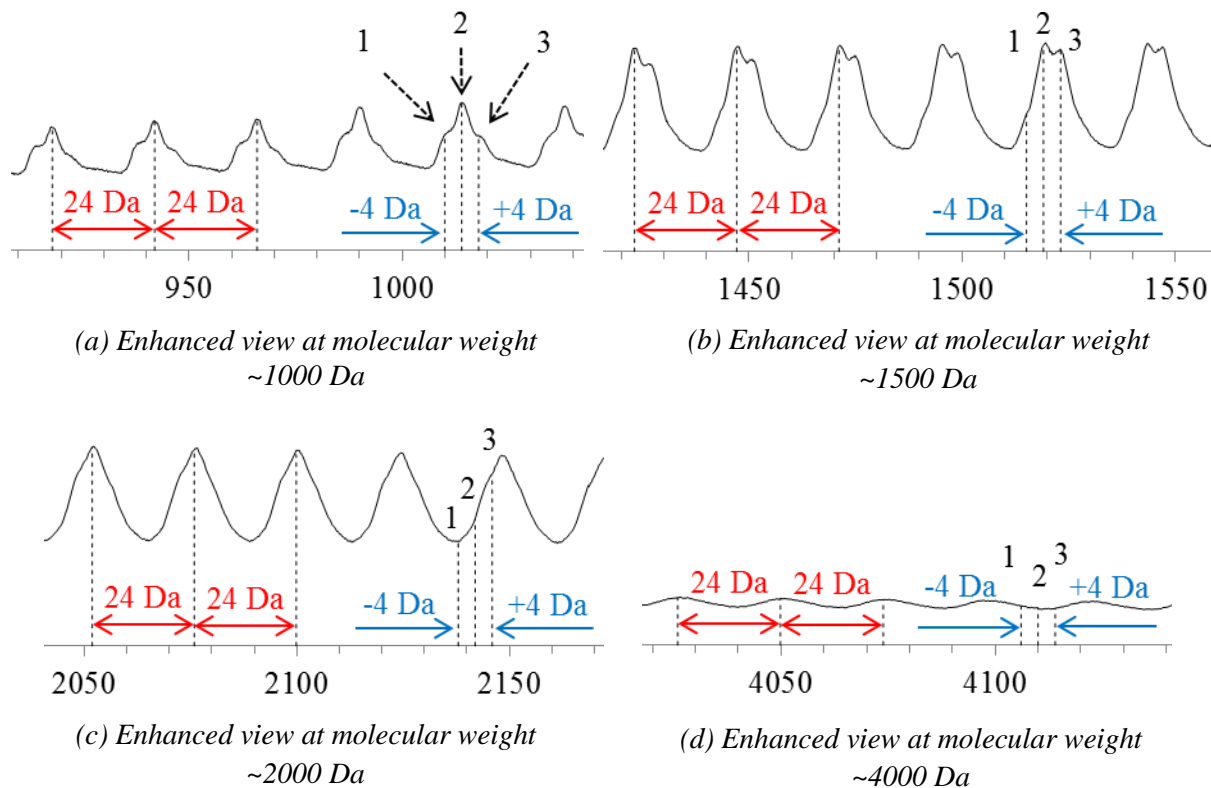
427

428

Figure 11: Incremental analysis on THF extract obtained at 450°C

429 **3.4.2 Solid coal**

430 Incremental analysis on solid state LDI-TOF-MS is shown in Figure 12a-d in enhanced views at ~1000,
 431 ~1500, ~2000, and ~4000 Da regions. For clarity, the spectral lines were presented as a continuous curve
 432 instead of discrete vertical lines.



433

434

Figure 12: Solid state LDI-TOF-MS incremental analysis on raw coal

435

436 The enhanced views presented from Figure 12a to Figure 12d shows that the bulk MWD of solid coal
 437 consisted of different peak groups which were separated by 24 Da increments. However, the shape of
 438 each 24 Da repeating peak comprised of a number of substantial sub-peaks which exhibited complex
 439 behaviour at higher molecular weight. Specifically, at about 1000 Da, a peak group could be considered
 440 to consist of three significant sub-peaks with a dominant second peak each separated by a 4 Da increment.
 441 At 1500 Da, the second and third sub-peaks had similar prominence. At 2000 Da the peak broadening
 442 became apparent with significant overlap between peaks, and eventually no distinguished peak could be
 443 observed at beyond 4000 Da. This was due to the decrease in resolving power of high mass compounds, a
 444 feature of LDI-TOF-MS instrument.

445 To perform incremental analysis throughout the coal spectrum, a peak group consisted of three local
446 peaks: peak 1, 2, and 3 (at 1034, 1038, and 1042 Da, respectively) were chosen from Figure 12a. The
447 corresponding MW of their peak family at higher molecular weight was obtained by adding these initial
448 values to multiples of 24 Da. These repeating multiples were 16, 46, and 128 to reach the molecular
449 weights in Figure 12b, c, and d, respectively. The calculated peak family at ~1500 Da (Figure 12b)
450 aligned well with the calculated peak positions. At ~2000 Da, none of the calculated peaks using
451 repeating number of 46 aligned with the obtained peak. In each case, the sub-peaks appeared to shift +2
452 Da away from the calculated values. At 4000 Da this shift increased to about +8 Da. Clearly, this
453 observed phenomenon in the coal's structure is complex and further work is required to understand its
454 molecular importance.

455 **4 Discussion**

456 *4.1 The role of volatiles in driving swelling*

457 Volatile evolution was measured with the DETA technique as a mixture of volatile tars and light gases.³⁴
458 ³⁵ When combined with the thermo-physical measurements from the CATA technique, it was found that
459 tar evolution was closely associated with coal swelling behaviour. This was evident in the dominance of
460 generated volatile tar over light gases evolution within the swelling range (Table 5) and the similar
461 temperatures of peak tar release with maximum swelling rate (Table 2 and Table 4). However, tar
462 evolution was shown to occur over a much wider temperature range than the thermoplastic region. This
463 clearly suggests a more complex relationship exists between volatiles driving swelling and overall
464 thermoplastic behaviour.

465 The onset of light gas evolution was found to occur at similar temperature to swelling onset. Light gases
466 have previously been linked with cross-linking mechanisms and are commonly included together in
467 pyrolysis models such as FLASHCHAIN,¹⁴ FG – DVC,¹⁵ and CPD¹⁶. A plausible explanation for this
468 complex process may be that the tar evolution is indicative of semi-volatile materials that are capable of

469 adding to the fluid forming material during the plastic phase and that the light gases can act as the driver
470 for swelling. In the thermoplastic range (430-482°C), tar evolution accounted for 84% of the total
471 volatiles release (in terms of mass of carbon), compared to just ~16% in the case of light gases. However,
472 the condensable tars measured a peak molecular weight at ~250-350 Da which extended up to 500 Da.
473 Such a molecular size is consistent with 5-7 ringed aromatics with much higher boiling temperatures such
474 as benzo(a)pyrene (5 rings, 252 Da, boiling point 495°C) or coronene (7 rings, 300 Da, boiling point
475 525°C). The outcome of these combined measurements suggests that actual *volumetric* flow of volatile
476 tars is low despite the *mass* flow rate being greater than light gases. As an estimate, the volumetric
477 contribution of tars (as coronene 300 Da) and light gas (as CH₄) to swelling was calculated as 18% and
478 82%, respectively. This difference in volumetric flow supports the delay between the measured softening
479 (from ΔP) and swelling, in that the release of tars after softening provides insufficient driving force
480 without the evolution of light gas.

481 **4.2 Molecular changes in pyrolysis products during coking**

482 Pyrolysis products, both vaporised and solvent-extractable components from the semi-coke, were
483 obtained through pre-heating coal to a suite of temperatures that covered the plastic range. The volatile
484 component had the lowest molecular range, with an upper limit of 400-600 Da. This upper-limit of 600
485 Da was small compared to previous work which reported up to ~1000 Da molecular sizes under rapid
486 heating conditions (~1000°C/s).⁴¹ The explanation for this might simply be that different coals were used
487 in two studies, or that the slow heating rate in this study may have allowed a certain retention time of
488 volatile tar inside the coal particle,⁴⁴ which can lead to greater extent of secondary reactions between
489 escaping tar and the solid residue⁴⁵.

490 With respect to solvent soluble components, this work has shown that the molecular weight distribution
491 of the raw coal extractable materials is similar to that of extracts up to 350°C, while further increases in
492 temperature results in significant structural changes that coincide with a “bulk” thermoplastic response
493 (i.e., softening and swelling). This thermoplastic behaviour corresponded to an observed increase in

494 molecular size of the solvent-soluble components, particularly in the range of 500-1800 Da, which
495 subsequently disappeared on resolidification. This change in molecular character of the solvent extracts
496 along with the consistent increase in MWD of volatile tar clearly suggests depolymerisation of coal
497 structure to form smaller fragments, consistent with the pyrolysis mechanisms described in
498 FLASHCHAIN,¹⁴ FG-DVC,¹⁵ and CPD¹⁶ models.

499 Detailed incremental analysis on the pyrolysis products obtained at 450°C showed that there was a
500 repetition of peak series separated by 12-14 Da on volatile and solvent extracts, particularly at MW <600
501 Da. These results agree well with previous works on tar conducted by Herod et al.⁴¹ and Nomura et al.⁴³,
502 or on solvent extraction of semi-coke performed by Stanger et al.⁴⁰. In addition, it was found that position
503 of peaks in this particular MW range appeared to align well between vaporised (volatile tar) and <600 Da
504 components in acetone and THF extracts. This alignment indicates a similarity in their chemical structure
505 consistent with a tar vaporisation mechanism as explained by Unger and Suuberg⁴⁶ (as opposed to a tar
506 cracking mechanism). Under this scenario, tar species could be formed during pyrolysis and yet remain
507 within the coal structure prior to vaporising. This tar retention would lead to a build-up of semi-volatile
508 material that could contribute towards fluid development.

509 For compounds with MW higher than 600 Da, there appeared an additional 24 Da repeating structure in
510 THF extract spectrum. This 24-Da repeating unit (e.g., an ethylene structure $-C\equiv C-$) has been implicated
511 in soot formation,⁴⁷ and has been suggested as a key decomposition pathway in coal pyrolysis⁴⁸. Further
512 heating led to the disappearance of these compounds. At 500°C, THF extract spectrum possessed a
513 similar MWD compared to the collected volatile tar. This suggests that the 500-1800 Da molecular
514 structures are a key intermediate in the formation of a thermoplastic phase, and that material <500 Da are
515 not able to independently form this phase alone. This temperature, interestingly, was close to the peak in
516 light gas evolution (at 494°C). Such observation in light gases production between 400-500°C fits with
517 moderate-temperature cross-linking mechanism that occurs after tar evolution reaches its maxima, as
518 described by Deshpande et al.⁴⁹ and Solomon et al.^{50,51}.

519 4.3 Solid state LDI-TOF-MS

520 Solid state LDI-TOF-MS has been applied to solid coal particles by several researchers including the
521 Argonne Premium Coal Suite,⁵² maceral rich coals,⁵³ and as a form of image analysis⁵⁴. This work has
522 measured comparable molecular range to that of Herod et al.⁵² and Stanger et al.⁵⁴ for similar reflectance
523 coals. Further incremental analysis was conducted on different regions in coal MW spectrum to gain
524 better understanding of coal chemical structure rather than just focusing on determining the largest
525 molecular size in coal (as in Herod et al.⁵²). The coal spectrum contained a series of peak groups
526 separated by 24 Da spacing, similar to >600 Da region recorded in THF extract spectrum. Importantly,
527 the observed 12-14 Da repeating structure in MW spectra of volatile tar, acetone extract, and THF extract
528 at MW <600 Da region was not apparent in the raw coal, indicating the importance of the pyrolysis
529 process in producing these fractions and the complexities involved in the structure of coal.

530

531 5 Conclusions

532 A number of analytical techniques (CATA, TGA, DETA, and LDI-TOF-MS) were utilised to study
533 thermoplastic properties of one Australian coking coal. Bulk changes were measured via its thermal
534 volumetric expansion and volatiles release (including tar and light gases evolution). Molecular changes
535 were measured in condensed volatile tar and solvent extracts from heated semi-cokes and compared to
536 that of the solid coal. Results of this present work are:

- 537 • Both the mobile phase (solvent extractable materials in raw coal) and the metaplast (heat-
538 generated materials) contributed to coking coal swelling property. Although the removal of the
539 mobile phase led to a dramatic reduction in thermal swelling capacity, the metaplast was found to
540 be mainly responsible for coal swelling behaviour.

- 541 • The majority of volatile release within the thermo-swelling range was measured as tar evolution.
542 However, the commencement of swelling phenomenon was found to be closer to the onset of
543 light gases release.
- 544 • The observed thermo-physical changes within the plastic range were found to be reflected in the
545 changes in molecular structures of the pyrolysis products. In particular, the appearance and
546 subsequent disappearance of 500-1800 Da material with 24 Da repeating structure closely
547 followed the development of the thermoplastic process.
- 548 • The molecular weight distribution of raw coal extended beyond 7000 Da and was much broader
549 compared to its tar and solvent extracts. The spectrum was found to consist of multiple repeating
550 peak groups separated by 24 Da, similar to the reoccurring pattern found in solvent extract at MW
551 higher than 600 Da.

552

553 **Acknowledgement**

554 The authors gratefully acknowledge the Australian Research Council for funding this work under project
555 DP140104185. The authors would also like to acknowledge the University of Newcastle's Analytical and
556 Biomolecular Research Facility (ABRF) for their use of mass spectrometry unit and technical staff. Tran
557 would like to thank the financial support from the University of Newcastle for his Ph.D. scholarship
558 under the UNRSC 50:50 scheme.

559 **References**

- 560 1. Loison, R.; Foch, P.; Boyer, A., *Coke: Quality and Production*. Butterworths: 1989.
561 2. Díez, M. A.; Alvarez, R.; Barriocanal, C., Coal for metallurgical coke production: predictions of
562 coke quality and future requirements for cokemaking. *International Journal of Coal Geology* **2002**, 50,
563 (1–4), 389-412.
564 3. Gill, W. W.; Chaklader, A. C. D., Material characteristics affecting formcoke. *Fuel* **1984**, 63,
565 (10), 1385-1392.

- 566 4. Lucht, L. M.; Peppas, N. A., Macromolecular structure of coals: 2. Molecular weight between
567 crosslinks from pyridine swelling experiments. *Fuel* **1987**, 66, (6), 803-809.
- 568 5. Marzec, A.; Kisielow, W., Mechanism of swelling and extraction and coal structure. *Fuel* **1983**,
569 62, (8), 977-979.
- 570 6. Van Krevelen, D. W., *Coal: Typology, Physics, Chemistry, Constitution*. Elsevier: 1993.
- 571 7. Nishioka, M., The associated molecular nature of bituminous coal. *Fuel* **1992**, 71, (8), 941-948.
- 572 8. Davidson, R. M., Molecular Structure of Coal. In *Coal Science*, Wender, M.; Gorbatyjohn, L.;
573 Larsenirving, W., Eds. Academic Press: 1982; pp 83-160.
- 574 9. Solomon, P. R., Coal Structure and Thermal Decomposition. In *New Approaches in Coal*
575 *Chemistry*, ACS Symposium Series: 1981; Vol. 169, pp 61-71.
- 576 10. Jüntgen, H., Coal Characterization in Relation to Coal Combustion. In *Fundamentals of the*
577 *Physical-Chemistry of Pulverized Coal Combustion*, Lahaye, J.; Prado, G., Eds. Springer Netherlands:
578 1987; Vol. 137, pp 4-58.
- 579 11. Given, P. H., An Essay on the Organic Geochemistry of Coal. In *Coal Science*, Wender, M. L. G.
580 W. L., Ed. Academic Press: 1984; pp 63-252.
- 581 12. Wilhelm, A.; Hedden, K., A non-isothermal experimental technique to study coal extraction with
582 solvents in liquid and supercritical state. *Fuel* **1986**, 65, (9), 1209-1215.
- 583 13. Akash, B. A., Thermochemical liquefaction of Coal. *Int. J. of Thermal & Environmental*
584 *Engineering* **2013**, 5, (1).
- 585 14. Niksa, S., Rapid coal devolatilization as an equilibrium flash distillation. *AIChE Journal* **1988**,
586 34, (5), 790-802.
- 587 15. Solomon, P. R.; Hamblen, D. G.; Serio, M. A.; Yu, Z.-Z.; Charpenay, S., A characterization
588 method and model for predicting coal conversion behaviour. *Fuel* **1993**, 72, (4), 469-488.
- 589 16. Grant, D. M.; Pugmire, R. J.; Fletcher, T. H.; Kerstein, A. R., Chemical model of coal
590 devolatilization using percolation lattice statistics. *Energy & Fuels* **1989**, 3, (2), 175-186.
- 591 17. Solomon, P. R.; Hamblen, D. G.; Yu, Z.-Z.; Serio, M. A., Network models of coal thermal
592 decomposition. *Fuel* **1990**, 69, (6), 754-763.
- 593 18. Pajares, J. A.; DiezDíez, M. A., Coal and Coke. In *Encyclopedia of Analytical Science (Second*
594 *Edition)*, Worsfold, P.; Townshend, A.; Poole, C., Eds. Elsevier: Oxford, 2005; pp 182-197.
- 595 19. Nomura, S.; Thomas, K. M., Fundamental aspects of coal structural changes in the thermoplastic
596 phase. *Fuel* **1998**, 77, (8), 829-836.
- 597 20. Gray, R. J., Coal to Coke Conversion. In *Introduction to Carbon Science*, Edwards, H. M. A. S.;
598 Menendez, R.; Rand, B.; West, S.; Hosty, A. J.; Kuo, K.; McEnaney, B.; Mays, T.; Johnson, D. J.;
599 Patrick, J. W.; Clarke, D. E.; Crelling, J. C.; Gray, R. J., Eds. Butterworth-Heinemann: 1989; pp 285-321.
- 600 21. Ouchi, K.; Itoh, S.; Makabe, M.; Itoh, H., Pyridine extractable material from bituminous coal, its
601 donor properties and its effect on plastic properties. *Fuel* **1989**, 68, (6), 735-740.
- 602 22. Chermin, H. A. G.; Van Krevelen, D. W., Chemical structure and properties of coal. XVII. A
603 mathematical model of coal pyrolysis. *Fuel* **1957**, 36, 85-104.
- 604 23. Fitzgerald, D., The kinetics of coal carbonization in the plastic state. *Transactions of the Faraday*
605 *Society* **1956**, 52, (0), 362-369.
- 606 24. Oh, M. S.; Peters, W. A.; Howard, J. B., An experimental and modeling study of softening coal
607 pyrolysis. *AIChE Journal* **1989**, 35, (5), 775-792.
- 608 25. Smith, K. L.; Smoot, L. D.; Fletcher, T.; Pugmire, R., Devolatilization Rate Processes and
609 Products. In *The Structure and Reaction Processes of Coal*, Springer US: 1994; pp 209-323.
- 610 26. Takanohashi, T.; Yoshida, T.; Iino, M.; Kato, K.; Fukade, K.; Kumagai, H., Structural Changes of
611 Coal Macromolecules During Softening. In *Structure and thermoplasticity of coal* Komaki, I.; Itagaki, S.;
612 Miura, T., Eds. Nova Science Publishers: 2005.
- 613 27. Miura, K.; Tomobe, H.; Fujisawa, T.; Komatsu, Y.; Uebo, K., Quantitative Estimation of
614 Metaplast in Heat-Treated Coal by Solvent Extraction. In *Structure and Thermoplasticity of Coal*,
615 Komaki, I.; Itagaki, S.; Miura, T., Eds. Nova Science Publishers: 2005.

616 28. Takanohashi, T.; Yoshida, T.; Iino, M.; Katoh, K.; Fukada, K., Effect of heavy solvent-soluble
617 Constituents on Coal Fluidity. *Energy & Fuels* **1998**, 12, (5), 913-917.

618 29. International Organization for Standardization (ISO), ISO 7404-5: Methods for the petrographic
619 analysis of coals - Part 5: Method of determining microscopically the reflectance of vitrinite. In *ISO/TC*
620 *27/SC 5 - Methods of analysis*, 2009.

621 30. Ballantyne, T. R.; Ashman, P. J.; Mullinger, P. J., A new method for determining the conversion
622 of low-ash coals using synthetic ash as a tracer. *Fuel* **2005**, 84, (14-15), 1980-1985.

623 31. Xie, W.; Stanger, R.; Wall, T. F.; Lucas, J. A.; Mahoney, M. R., Associations of physical,
624 chemical with thermal changes during coking as coal heats - Experiments on coal maceral concentrates.
625 *Fuel* **2015**, 147, 1-8.

626 32. Xie, W.; Stanger, R. J.; Lucas, J.; Mahoney, M.; Elliott, L. K.; Yu, J.-L.; Wall, T. F., Thermo-
627 swelling properties of particle size cuts of coal maceral concentrates. *Energy & Fuels* **2015**, 29, (8),
628 4893-4901.

629 33. Xie, W.; Stanger, R.; Lucas, J.; Wall, T.; Mahoney, M., Coal macerals separation by reflux
630 classification and thermo-swelling analysis based on the Computer Aided Thermal Analysis. *Fuel* **2013**,
631 103, (0), 1023-1031.

632 34. Stanger, R.; Xie, W.; Wall, T.; Lucas, J.; Mahoney, M., Dynamic Elemental Thermal Analysis: A
633 technique for continuous measurement of carbon, hydrogen, oxygen chemistry of tar species evolved
634 during coal pyrolysis. *Fuel* **2013**, 103, (0), 764-772.

635 35. Stanger, R.; Wall, T.; Lucas, J.; Mahoney, M., Dynamic Elemental Thermal Analysis (DETA) –
636 A characterisation technique for the production of biochar and bio-oil from biomass resources. *Fuel* **2013**,
637 108, 656-667.

638 36. Stanger, R.; Xie, W.; Wall, T.; Lucas, J.; Mahoney, M., Dynamic measurement of coal thermal
639 properties and elemental composition of volatile matter during coal pyrolysis. *Journal of Materials*
640 *Research and Technology* **2014**, 3, (1), 2-8.

641 37. Marzec, A.; Juzwa, M.; Betlej, K.; Sobkowiak, M., Bituminous coal extraction in terms of
642 electron-donor and -acceptor interactions in the solvent/coal system. *Fuel Processing Technology* **1979**, 2,
643 (1), 35-44.

644 38. Fletcher, T. H.; Kerstein, A. R.; Pugmire, R. J.; Solum, M. S.; Grant, D. M., Chemical percolation
645 model for devolatilization. 3. Direct use of carbon-13 NMR data to predict effects of coal type. *Energy &*
646 *Fuels* **1992**, 6, (4), 414-431.

647 39. Mullins, O. C., The modified Yen Model. *Energy & Fuels* **2010**, 24, (4), 2179-2207.

648 40. Stanger, R.; Borrowdale, J.; Smith, N.; Xie, W.; Tran, Q. A.; Lucas, J.; Wall, T., Changes in
649 solvent-extracted matter for heated Coal during Metaplast Formation Using High-Range Mass
650 Spectrometry. *Energy & Fuels* **2015**, 29, (11), 7101-7113.

651 41. Herod, A. A.; Li, C.-Z.; Xu, B.; Parker, J. E.; Johnson, C. A. F.; John, P.; Smith, G. P.;
652 Humphrey, P.; Chapman, J. R.; Kandiyoti, R.; Games, D. E., Characterization of coal by matrix-assisted
653 laser desorption mass spectrometry. II. Pyrolysis tars and liquefaction extracts from the argonne coal
654 samples. *Rapid Communications in Mass Spectrometry* **1994**, 8, (10), 815-822.

655 42. Rodgers, R. P.; Marshall, A. G., Petroleomics: Advanced Characterization of Petroleum-Derived
656 Materials by Fourier Transform Ion Cyclotron Resonance Mass Spectrometry (FT-ICR MS). In
657 *Asphaltenes, Heavy Oils, and Petroleomics*, Mullins, O. C.; Sheu, E. Y.; Hammami, A.; Marshall, A. G.,
658 Eds. Springer New York: New York, NY, 2007; pp 63-93.

659 43. Nomura, M.; Kidena, K.; Murate, S.; Yoshida, S.; Nomura, S., Molecular Structure and
660 Thermoplastic Properties of Coal. In *Structure and thermoplasticity of coal*, Komaki, I.; Itagaki, S.; Miura,
661 T., Eds. Nova Science Publishers: 2005; pp 1-34.

662 44. Gavalas, G. R., Heat and mass transfer in pyrolysis. In *Coal pyrolysis*, Elsevier Scientific
663 Publishing: Amsterdam; the Netherlands, 1982; pp viii, 168 p.

664 45. Peters, W. A., Studies of the Pyrolysis Behavior of Condensed phase fuels with applications to
665 fuel conversion technology. In *Analytical Pyrolysis*, Voorhees, K. J., Ed. Butterworth-Heinemann: 1984;
666 pp 349-406.

- 667 46. Unger, P. E.; Suuberg, E. M., Molecular weight distributions of tars produced by flash pyrolysis
668 of coals. *Fuel* **1984**, 63, (5), 606-611.
- 669 47. Richter, H.; Howard, J. B., Formation of polycyclic aromatic hydrocarbons and their growth to
670 soot—a review of chemical reaction pathways. *Progress in Energy and Combustion Science* **2000**, 26, (4–
671 6), 565-608.
- 672 48. Solomon, P. R.; King, H.-H., Tar evolution from coal and model polymers: Theory and
673 experiments. *Fuel* **1984**, 63, (9), 1302-1311.
- 674 49. Deshpande, G. V.; Solomon, P. R.; Serio, M. A., Crosslinking reactions in coal pyrolysis.
675 *Preprint, Am. Chem. Soc., Div. Fuel Chem.* **1988**, 33, (2), 310-321.
- 676 50. Solomon, P. R.; Hamblen, D. G.; Carangelo, R. M.; Serio, M. A.; Deshpande, G. V., General
677 model of coal devolatilization. *Energy & Fuels* **1988**, 2, (4), 405-422.
- 678 51. Solomon, P. R.; Serio, M. A.; Deshpande, G. V.; Kroo, E., Cross-linking reactions during coal
679 conversion. *Energy & Fuels* **1990**, 4, (1), 42-54.
- 680 52. Herod, A. A.; Li, C.-Z.; Parker, J. E.; John, P.; Johnson, C. A. F.; Smith, G. P.; Humphrey, P.;
681 Chapman, J. R.; Kandiyoti, R.; Games, D. E., Characterization of coal by matrix-assisted laser desorption
682 ionization mass spectrometry. I. The Argonne coal samples. *Rapid Communications in Mass*
683 *Spectrometry* **1994**, 8, (10), 808-814.
- 684 53. Van Niekerk, D.; Pugmire, R. J.; Solum, M. S.; Painter, P. C.; Mathews, J. P., Structural
685 characterization of vitrinite-rich and inertinite-rich Permian-aged South African bituminous coals.
686 *International Journal of Coal Geology* **2008**, 76, (4), 290-300.
- 687 54. Stanger, R.; Tran, Q. A.; Xie, W.; Smith, N.; Lucas, J.; Yu, J.; Kennedy, E.; Stockenhuber, M.;
688 Wall, T., The use of LDI-TOF imaging mass spectroscopy to study heated coal with a temperature
689 gradient incorporating the plastic layer and semi-coke. *Fuel* **2016**, 165, 33-40.

690

691